Cancer Chemother Pharmacol (1998) 42: 183–193

ORIGINAL ARTICLE

Steven R. Meikle · Julian C. Matthews
Cathryn S. Brock · Paula Wells · Robert J.A. Harte
Vincent J. Cunningham · Terry Jones · Pat Price

Pharmacokinetic assessment of novel anti-cancer drugs using spectral analysis and positron emission tomography: A feasibility study

Received: 12 May 1997 / Accepted: 4 February 1998

Abstract *Purpose*: The aim of this study was to investigate the feasibility of evaluating the pharmacokinetics of radiolabeled anti-cancer drugs using spectral analysis, a non-compartmental tracer kinetic modeling technique, and positron emission tomography (PET). *Methods*: Dynamic PET studies were performed on patients receiving tracer doses of 5-fluorouracil (5-[^{18}F]-FU) and two developmental drugs – [^{11}C]-temozolomide and [^{11}C]-acridine carboxamide. Spectral analysis was then used to (a) determine individual and group average pharmacokinetics, (b) predict tumour handling in response to different drug administration regimens, and (c) produce functional parametric images describing regional pharmacokinetics. *Results*: Spectral analysis could distinguish tumour kinetics from normal tissue kinetics in an individual [^{11}C]-temozolomide study and demonstrated a markedly greater volume of distribution (VD) in glioma than in normal brain, although there was no appreciable difference in mean residence time. Analysis of pooled acridine carboxamide data ($n = 22$) revealed a relatively large VD (and prolonged retention) in the liver and spleen and a markedly lower VD (and initial uptake) in the brain. Continuous infusion of 5-[^{18}F]-FU was predicted to achieve a concentration in colorectal metastases in liver approximately 10 times that achieved in plasma at 10 h after commencement of the infusion. *Conclusions*: We conclude that spectral analysis provides important pharmacokinetic information about radiolabeled anti-cancer drugs with relatively few model assumptions.

S.R. Meikle (✉)
PET and Nuclear Medicine Department,
Royal Prince Alfred Hospital, Missenden Road,
Camperdown, NSW 2050, Australia
Tel.: 61 2 9515 6173; Fax: 61 2 9515 6381;
e-mail: steve@nucmed.rpa.cs.nsw.gov.au

J.C. Matthews · C.S. Brock · P. Wells · R.J.A. Harte
V.J. Cunningham · T. Jones · P. Price
Postgraduate Medical School, Du Cane Road,
London W12 ONN, UK

Key words Positron emission tomography · Pharmacokinetics · Anti-cancer drugs · Drug evaluation · Spectral analysis

Introduction

Recent advances in molecular biology have identified specific cellular targets for cancer therapy, leading to novel strategies for drug design. However, the evaluation of new anti-cancer drugs in humans continues to rely on serial plasma measurements of drug concentration and clinical indicators of response and toxicity. Tumour and normal tissue kinetics are either inferred from plasma measurements or extrapolated from animal models. However, plasma data cannot reliably predict regional pharmacokinetics, and extrapolation from animal models may be inappropriate due to species specificity, particularly in relation to new drugs with novel mechanisms of action. Positron emission tomography (PET) offers a significant advance with its ability to follow directly the time course of radiolabeled drug in human tumours and normal tissues in vivo [24, 26].

The full potential of PET is realised when the observed time course of labeled drug in tissue can be related to the tracer concentration in plasma via an appropriate model. This enables the determination of rate constants of exchange between plasma and the tissue(s) of interest. The conventional approach is to construct a compartmental model, with each compartment representing a particular tissue space or chemical form of the compound. This requires some prior knowledge of the biological fate of the compound in vivo. Such models are highly constrained, with the number of compartments and the relationships between them being fixed. If the assumptions of the model are correct, the rates of exchange between compartments can be estimated, from which pharmacokinetic variables are derived. However, compartmental models are prone to bias and/or a poor fit to the measured data if the assumptions are incorrect. This is especially the case for heterogeneous tissues such

as human tumours. Furthermore, sufficient a priori knowledge is often unavailable when developmental drugs are studied in humans, especially at the phase I stage.

Spectral analysis is a general modeling approach that enables the determination of pharmacokinetic variables with relatively few model assumptions [8]. The observed time course of labeled drug is fitted with a linear combination of possible tissue response curves representing a wide range of expected kinetic behaviour. No assumption is made about the number of compartments present or the relationships between them. The technique allows kinetic components present in the measured data to be readily identified and, as a result, is less prone to bias than the more highly constrained compartmental models. Therefore, we believe that spectral analysis is ideally suited to the study of radiolabled novel anti-cancer drugs with PET. However, to data the technique has not been applied to this problem, nor have its limitations been defined.

In this paper we investigate the utility of spectral analysis and PET for pharmacokinetic evaluation of novel anti-cancer drugs in vivo. We first present the principles of spectral analysis and compare this technique with the more conventional compartmental modeling approach. We then describe the use of spectral analysis for (a) determination of individual and group average pharmacokinetics in tumours and normal tissues, (b) prediction of tumour handling in response to different drug administration regimens and (c) production of functional parametric images describing regional pharmacokinetics. The implementation, interpretation of results and limitations of the technique are discussed.

Materials and methods

Spectral analysis

The image data produced from a kinetic PET study comprise a sequential time series of tomographic images, typically acquired over 60–90 min. Each pixel value indicates the tracer concentration averaged over the interval (frame) during which the image was acquired. Tissue response or time-activity curves can be constructed by plotting of pixel values, or the mean of several pixels contained within a user-defined region of interest (ROI), against frame times. In addition to the PET images, the tracer concentration in arterial plasma is measured throughout the study. The problem, then, is to relate the tissue response curves, $C_{tiss}(t)$, to the tracer concentration in arterial plasma, $C_a(t)$, using an appropriate tracer kinetic model. In the spectral analysis method, C_{tiss} is modeled as a positive linear combination of basis functions, each of which is a single exponential in time convolved with C_a:

$$C_{tiss}(t) = \frac{1}{t_{i+1}-t_i}\int_{t_i}^{t_{i+1}} \left(\sum_{j=1}^{N} C_a(t) \otimes \alpha_j \exp\left(-\beta_j t\right)\right) \mathrm{d}t \quad \begin{array}{l}\alpha_j \geq 0 \\ \lambda \leq \beta_j \leq 1,\end{array} \tag{1}$$

where $\otimes$ denotes convolution, N is the maximal number of basis functions allowed in the model (typically 100), λ is the decay constant of the radioisotope and $t_i (i = 1,\ \mathrm{T})$ values are the frame times. The β values are chosen to cover the spectrum of expected kinetic behaviour, from the slowest possible clearance (λ) to the fastest measurable dynamic (e.g. 1 s^{-1}). C_{tiss} and C_a are not corrected for radioactive decay; hence, irreversible binding results in an apparent clearance of λ. Thus, the problem becomes one of determining the values of α that best fit the measured data given predefined β values (spaced logarithmically) on the interval $[\lambda, 1]$. We investigated alternative mappings and found parameter estimates to be relatively insensitive to the spacing of β values. Equation 1 can also be written in matrix notation as:

$$\underline{C_{tiss}} = \underline{\underline{A}}\,\underline{\alpha}, \tag{2}$$

where $\underline{C_{tiss}}$ is the measurement vector, $\underline{\alpha}$ is the solution vector, $\underline{\underline{A}}$ is a $T \times N$ matrix (T=number of time points) whose elements are given by:

$$A_{ij} = \frac{1}{t_{i+1}-t_i}\int_{t_i}^{t_{i+1}} C_a(t) \otimes \exp\left(-\beta_j t\right) \mathrm{d}t. \tag{3}$$

Equation 2 can be solved for $\underline{\alpha}$ using the non-negative least-squares (NNLS) algorithm [15], which is based on the weighted least-squares criterion:

$$\begin{aligned} &\text{Minimise } \Phi(\underline{\alpha}) = \left(\underline{\underline{A}}\,\underline{\alpha} - \underline{C_{tiss}}\right)^T \underline{\underline{W}}\left(\underline{\underline{A}}\,\underline{\alpha} - \underline{C_{tiss}}\right),\ \alpha \geq 0 \\ &\qquad\qquad \underline{\underline{W}} = \mathrm{cov}^{-1}(\underline{C_{tiss}}). \end{aligned} \tag{4}$$

In practice, $\underline{\underline{W}}$ is diagonal with $w_{ii} = \mathrm{var}^{-1}[C_{tiss}(t_i)]$ since PET measurements at each time point can be considered independent. Typically, only a small number of non-zero α values are obtained in the solution vector, corresponding to the smallest number of exponentials that adequately describe the data. For example, most PET data are adequately described by, at most, three spectral components due to noise and finite temporal sampling.

The fitted values of α, together with the corresponding chosen values of β, define the tissue unit impulse-response function:

$$h(t) = \sum_{j=1}^{N} \alpha_j \exp\left(-(\beta_j - \lambda)t\right), \tag{5}$$

from which pharmacokinetic parameters can be calculated as follows:

$$K_1 = h(0) = \sum_{j=1}^{N} \alpha_j \tag{6}$$

$$VD = \int_0^{\infty} h(t)\mathrm{d}t = \sum_{j=1}^{N} \frac{\alpha_j}{\beta_j - \lambda} \tag{7}$$

$$MRT = \frac{VD}{K_1}, \tag{8}$$

where K_1 is the rate constant for transport from plasma to tissue (equivalent to regional flow x extraction), VD is the fractional volume of distribution (i.e. the steady-state ratio of tracer concentrations in tissue and plasma) and MRT is the mean residence time of the tracer in the sampled tissue. Such parameters can be calculated for individual pixels, enabling the generation of functional parametric images that demonstrate both the kinetic behaviour and the spatial distribution of the drug [16]. In addition, images representing the impulse response at specified points in time can be produced, which are useful for describing the delivery or retention phases of drug uptake in tissue, depending on the chosen time point [10].

Assuming linear kinetics, it is also possible to predict the tissue response to any desired input by convolution of the given arterial input function with the unit impulse-response function. For example, it may be useful to predict the tissue response to a constant drug infusion. In this case, convolution of the impulse response function with a constant value is equivalent to integration of $h(t)$ with respect to time:

$$C_{tiss}(t) = R\int_0^t h(t)\mathrm{d}t$$
$$= R\sum_{j=1}^{N}\frac{\alpha_j}{\beta_j-\lambda}\left(1-\exp\left(-\left(\beta_j-\lambda\right)t\right)\right), \quad (9)$$

where R is the constant infusion rate $[C_a(t) = R]$. This approach is valid provided that the drug concentration in tissue remains sufficiently low that saturation of any of the observed kinetics does not occur.

Interpretation of results

Interpretation of results obtained with spectral analysis is best illustrated with an example using simulated kinetic data. A tissue curve was simulated by convolution of a typical arterial input function with the following function:

$$u(t) = 0.001\exp(-0.01t) + 0.001\exp(-0.001t), \quad (10)$$

and adding noise typical of a PET time-activity curve assuming Poisson statistics. Figure 1a shows the simulated noisy tissue curve and the model fit obtained by spectral analysis. Once one has determined the values of α that best fit the data (given predefined values of β), the results can be presented either as a unit impulse-response function (Fig. 1b) or as a spectrum of kinetic components (Fig. 1c). The impulse response function describes the time course of labeled compound that would be expected if it were possible to deliver the tracer instantaneously to the tissue. The spectrum reveals the number of kinetic components that adequately describe the data, with the speed of the dynamics increasing from left to right. In this case, two peaks were identified, corresponding approximately in position and amplitude to the fast and slow exponentials in the function of Eq. 10 (Fig. 1c).

The number of peaks appearing in the spectrum corresponds to the number of discrete tissue compartments that the PET technique can resolve. A peak appearing at the far left of the spectrum indicates complete trapping of the tracer in tissue, corresponding to $\beta = \lambda$ ($= 10^{-3.3}$ s $^{-1}$ for ^{11}C). A peak appearing at the far right indicates kinetics indistinguishable from the arterial input function, which may occur if blood vessels are included in the sampled ROI. Intermediate peaks represent tissue compartments that exchange reversibly either with plasma or with other tissue compartments. Thus, the spectrum provides an objective means of interpreting kinetic data and may be used to construct a specific compartmental model for further biological testing and analysis.

Fig. 1 **a** Simulated PET time-activity curve with Poisson noise added. **b** Unit impulse-response function obtained by spectral analysis of the curve shown in **a**. **c** The corresponding spectrum of kinetic components

Comparison with compartmental modeling

Tracer kinetics for a two-compartment system were simulated and analysed with both the spectral analysis method and conventional

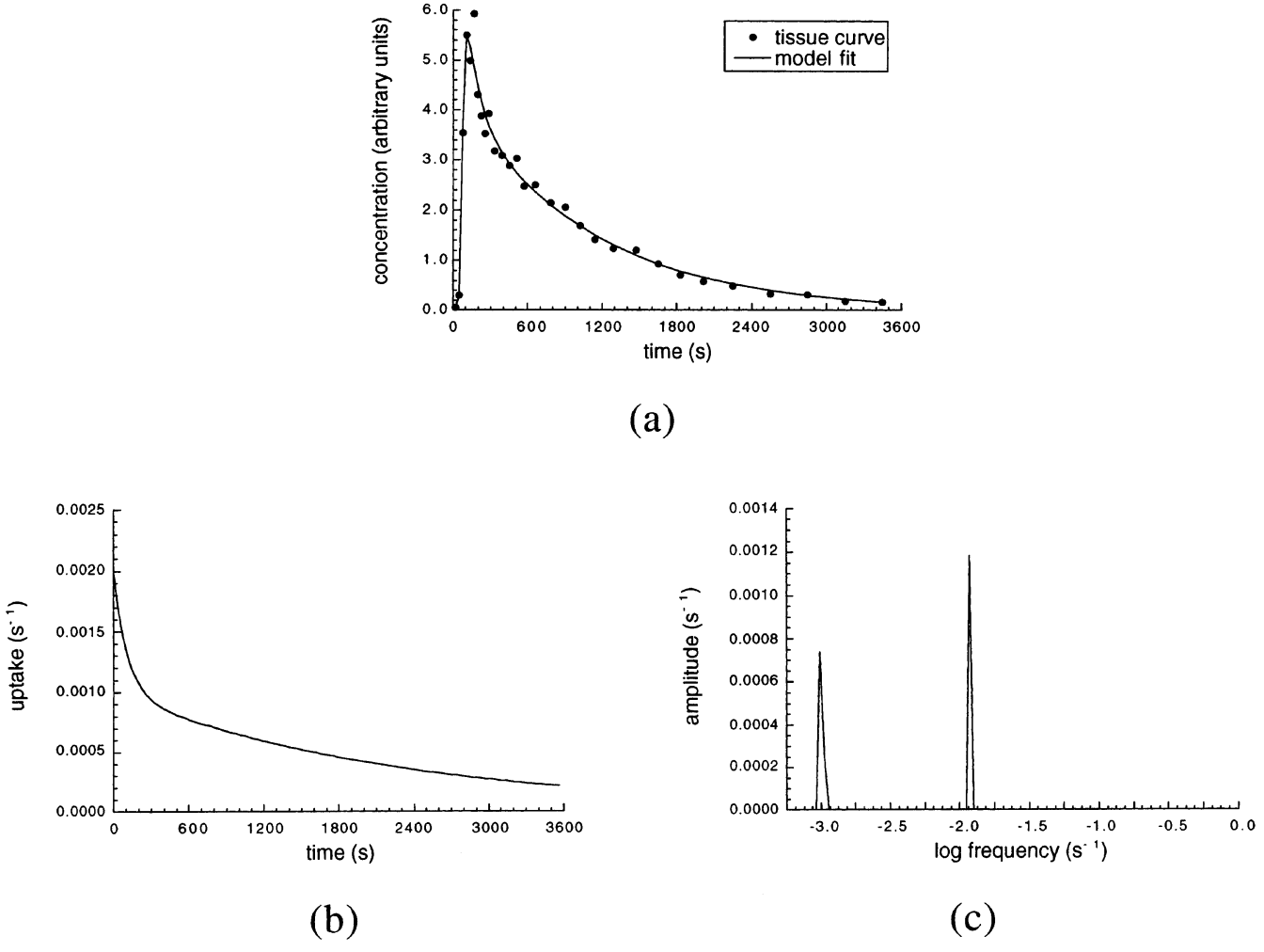

compartmental modeling. Tissue curves were generated by convolution of a typical arterial input function with the following impulse response function:

$$u(t) = 0.01\exp(-0.011t) + 0.005\exp(-0.0035t). \quad (11)$$

The resulting simulated tissue concentration curve was then averaged within each of 21 discrete intervals ranging from 5 s at the beginning to 600 s at the end. In all 100 such curves were generated, each time with the addition of Poisson noise with a different random seed, such that the noise level in each curve was 5% of the maximal signal, which is typical for a time-activity curve derived from a PET study acquired in the two-dimensional (2-D) mode. The curves were then analysed using spectral analysis with $N = 100$ basis functions and non-linear least-squares fitting, with the number of a priori tissue compartments being fixed at 2. The parameters K_1, *VD* and *MRT* were estimated by both methods for all 100 noisy curves, allowing evaluation of the accuracy and precision of parameter estimates.

Drugs investigated

The anti-cancer drugs chosen for this study included 5-fluorouracil (5-[^{18}F]-FU), a well-established anti-cancer drug in current routine clinical practice, and two developmental drugs being investigated by the UK Cancer Research Campaign (CRC): temozolomide (8-carbamoyl-3-methylimidazo[5,1-d]-1,2,3,5-tetrazin-4-(3H)-one) and acridine carboxamide {*N*-[2-(dimethylamine)ethyl]acridine-4-carboxamide}. Temozolomide is an oral cytotoxic prodrug that degrades in physiological solution to form the reactive methylating species MTIC [5-(3-methyltriazen-1-yl)imidazole-4-carboxamide], which is thought to achieve anti-tumour activity by binding to DNA guanine bases [23]. Temozolomide was labeled with ^{11}C in the 3-*N*-methyl position [5]. PET studies were conducted in parallel with a phase II clinical trial by the CRC. Acridine carboxamide is a third-generation drug that stimulates DNA cleavage by both topoisomerase I and topoisomerase II inhibition and is reported to be active against lung-tumour cell lines [1]. The drug was labeled with ^{11}C in the *N*-methyl position [4]. PET scans were performed in advance of phase I clinical trials by the CRC. All PET studies were approved by the Royal Postgraduate Medical School Research Ethics Committee and informed consent was obtained from each patient prior to inclusion in the study.

Data collection

[^{11}C]-Temozolomide studies were performed on a brain tomograph (ECAT 953B, Siemens/CTI, Knoxville, Tenn.) operated in the 3-D mode [22], whereas 5-[^{18}F]-FU and [^{11}C]-acridine carboxamide studies were performed on a whole-body tomograph (ECAT 931, Siemens/CTI, Knoxville, Tenn.) operated in the 2-D mode [21]. For [^{11}C]-temozolomide and [^{11}C]-acridine carboxamide studies, dynamic imaging continued for 90 min from the time of injection, whereas for 5-[^{18}F]-FU the study duration was 60 min. The image sequence comprised 21 frames for [^{11}C]-temozolomide studies (ranging from 5 to 600 s duration), 30 frames for 5-[^{18}F]-FU (30–300 s) and 32 frames (20–600 s) for [^{11}C]-acridine carboxamide.

Radioactivity in blood was measured at 1-s intervals throughout the PET studies via a radial artery catheter using a bismuth germanate counting system [19]. In addition, up to 12 discrete 5-ml blood samples were withdrawn from the same catheter at regular intervals. These were later analysed using high-performance liquid chromatography (HPLC) to determine the contribution of labeled metabolites to the total plasma radioactivity. The partitioning of radioactivity between plasma and whole blood was also determined by separate counting of plasma and whole blood in an NaI(TI) well counter. The on-line arterial measurements were corrected for plasma-to-whole-blood partitioning and the presence of labeled metabolites to obtain the plasma input function for spectral analysis.

Image reconstruction

Because of the increased contribution of scattered coincidences to 3-D PET measurements, the [^{11}C]-temozolomide data were corrected for scatter prior to image reconstruction [2]. Both 3-D and 2-D data were also corrected for attenuation of photons in the body using a ^{68}Ge/Ga transmission scan performed in the 2-D mode before tracer injection. The 2-D scans performed with 5-[^{18}F]-FU and [^{11}C]-acridine carboxamide were reconstructed using conventional filtered back-projection [18] to form 15 transaxial image planes spaced 6.75 mm apart. The 3-D [^{11}C]-temozolomide data were reconstructed using 3-D filtered back-projection [14] to form 31 transaxial image planes spaced 3.375 mm apart. For the 3-D studies the reconstructed spatial resolution is approximately 6 mm in the transverse plane (within slices) and 5 mm in the axial plane (between slices). For the 2-D studies the spatial resolution is approximately 8 mm in both the transverse and axial planes.

Applications of spectral analysis

Assessment of tumour and normal tissue pharmacokinetics

To illustrate the use of spectral analysis to assess pharmacokinetics in an individual, the technique was applied to data obtained from a [^{11}C]-temozolomide study performed on a 65-year-old woman with a high-grade astrocytoma. The patient was scheduled to receive oral temozolomide at therapeutic dose but was off treatment at the time of the PET scan. A 239-MBq (1.2-μg) dose of [^{11}C]-temozolomide was given intravenously. Following data collection and image reconstruction, regions of interest (ROI) were drawn over the tumour rim and an area of normal cortical grey matter on the contra-lateral side. Time-activity curves were calculated for each ROI and fitted with the spectral analysis model using the metabolite-corrected arterial input function. This allowed the unit impulse-response functions for tumour and normal brain tissue to be derived, from which pharmacokinetic variables were calculated.

Group average pharmacokinetics

PET scans were performed on 22 patients receiving between 175 and 667 MBq (mean 465 MBq) of [^{11}C]-acridine carboxamide intravenously, corresponding to drug doses of 4.6–18.5 μg. This dose range can be compared with the phase I starting dose of 18 mg m^{-2}. The scan data were acquired and images reconstructed as described above. Then, ROIs were defined on the images for a range of normal tissues and tumours and corresponding time-activity curves were calculated. These were fitted with the spectral analysis model using the metabolite-corrected arterial input function. The spectra were grouped according to common tissue types and averaged across patients by calculation of the mean amplitude for each dynamic in the spectral range $\lambda \leq \beta \leq 1$. These average spectra define average impulse response functions for each of the tissues sampled, which allows the determination of group-average pharmacokinetic variables.

Predicting drug handling by tumours

Previous work suggests that the pharmacokinetics of 5-[^{18}F]-FU are linear when the drug is given as a slow infusion [7, 11]. Therefore, it is feasible to extrapolate the results obtained by spectral analysis of a 5-[^{18}F]-FU tracer study to the case of a prolonged venous (constant) infusion of 5-[^{18}F]-FU. The patient studied was a 54-year-old woman with liver metastases from a colorectal primary tumour. A 349-MBq dose of 5-[^{18}F]-FU (13.8 mg) was given intravenously to the patient as a bolus. Following data collection and image reconstruction, an ROI was defined over a tumour in the liver. The unit impulse response was determined using spectral analysis and the metabolite-corrected arterial input function. The estimated parameters of the impulse response

Table 1 Parameter estimates obtained using spectral analysis and compartmental modeling

	Nominal value	Spectral analysis	2-Compartment model	1-Compartment model
K_1 (s^{-1})	0.015	0.0159 ± 0.0025	0.0154 ± 0.0016	0.0130 ± 0.0007
VD	2.34	2.33 ± 0.07	2.34 ± 0.03	2.30 ± 0.04
MRT (s)	156	149 ± 19	153 ± 14	178 ± 10

function were then substituted into Eq. 9 for determination of the tumour handing in response to a constant drug infusion.

Parametric images of pharmacokinetic variables

To illustrate the use of spectral analysis at an image pixel level, parametric images were calculated for the [^{11}C]-temozolomide study described above. Parametric images of *VD* and the impulse response at an early (1 min) and late (60 min) time point were calculated. The *VD* image was calculated by integration of the impulse response curve between time zero and the end of the PET study rather than extrapolation to infinity as the definition of *VD* requires. This is because the impulse response becomes increasingly unreliable for time points extrapolated beyond the end of the scan, resulting in noisy estimates of *VD*. Similarly, the 1-min time point was chosen to avoid problems in estimating the zero intercept of the impulse response function due to noise and vascular effects.

Results

Comparison with compartmental modeling

The mean and standard deviation of parameter estimates obtained with spectral analysis and compartment modeling of the simulated noisy tissue curves are given in Table 1. There was good agreement between estimated and nominal parameter values for both spectral analysis and the two-compartment model, although the bias in estimating K_1 and, hence, *MRT* was slightly higher for spectral analysis (6% versus 3%). The precision of parameter estimates was also slightly worse for spectral analysis. However, both the bias and the precision of parameter estimates with spectral analysis are acceptable, given that the model makes no assumption about the number of compartments present, whereas the compartmental model is more highly constrained. It should be noted that in the case of compartmental modeling this experiment represents an idealised situation where the number of tissue compartments are exactly known in advance. In practice the number of compartments may be unknown, particularly in the case of labeled developmental drugs, or may be obscured by the mixture of heterogeneous kinetics with an ROI. Therefore, it is pertinent that one also compare the results obtained when a single tissue compartment is assumed instead of two, shown in the last column of Table 1. In this case the bias in estimation of K_1 becomes −13%.

Assessment of tumour and normal tissue pharmacokinetics

A representative image of the cumulative [^{11}C]-temozolomide uptake over 90 min is shown in Fig. 2a, together with the derived time-activity curves generated for plasma, normal cortical grey matter and tumour rim (Fig. 2b). The spectra suggest that there are three exponentials present in tumour kinetics, whereas temozolomide uptake in normal brain is adequately described by just two exponentials (Fig. 2c). Reversible compartments are present in both tumour and normal brain, as indicated by the peaks lying near $\log\beta = -1.5$ and $\log\beta = -2.5$, as is a nearly irreversible compartment that is very similar in position and amplitude for tumour and normal brain. Note that completely irreversible ligand binding would result in a peak at $\log\beta = -3.3$, corresponding to radioactive decay of ^{11}C ($\lambda = 0.00056\ s^{-1}$). The impulse response functions suggest that the main differences in drug handling by the brain and tumour occur in the first 15 min of uptake (Fig. 2d). This is reflected in the K_1 estimates for the two tissues, which indicate approximately 7-fold greater uptake from plasma into tumour than into normal brain (Table 2). After approximately 30 min the kinetic behaviour of temozolomide in tumour and normal grey matter is almost indistinguishable. Consequently, the terminal half-clearance ($t_{1/2z}$) values are very similar, although a slightly prolonged clearance from tumour (approx. 20%) can be noted. This analysis suggests that the increased accumulation of temozolomide into tumour as compared with normal brain tissue is mainly due to increased drug delivery. This is probably due to breakdown of the blood-brain barrier [3]. Small differences in drug binding between tumour and normal brain may also exist.

Group average pharmacokinetics

Average spectra and corresponding impulse response functions for the phase I drug acridine carboxamide in normal tissue (lung parenchyma) and various tumours are shown in Fig. 3. Pharmacokinetic parameter estimates for all tissues sampled are given in Table 3. The spectra of Fig. 3a suggest three reasonably distinct kinetic components for lung parenchyma – two reversible compartments and one irreversible or very slowly clearing compartment (also seen in the impulse response function of Fig. 3c). The tumour spectrum (Fig. 3b) is more heterogeneous, reflecting the range of tumours sampled. However, there is nonetheless a strong suggestion of an irreversible or very slowly clearing compartment and, possibly, two reversible compartments. The peak adjacent to the blood volume component at $\log\beta = 0$ is most likely due to delay and/or dispersion of the measured input function relative to the actual arterial blood supply.

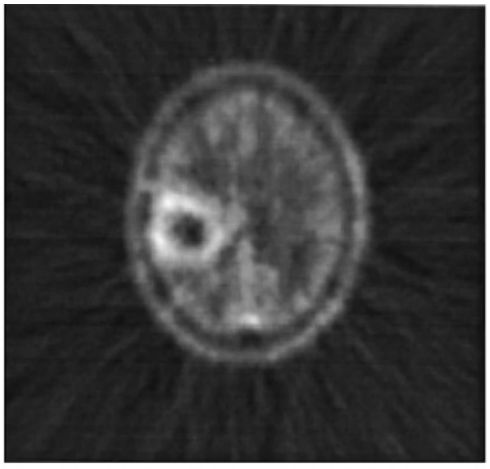

(a)

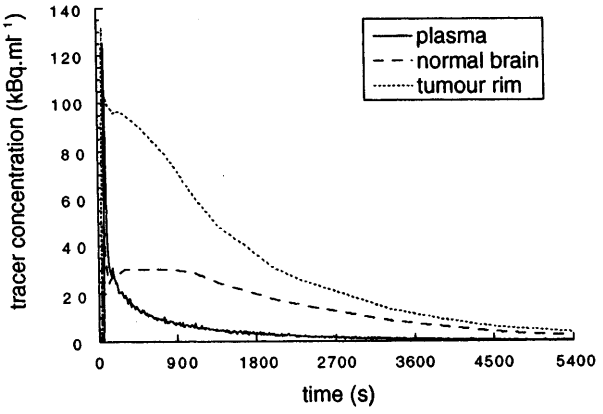

(b)

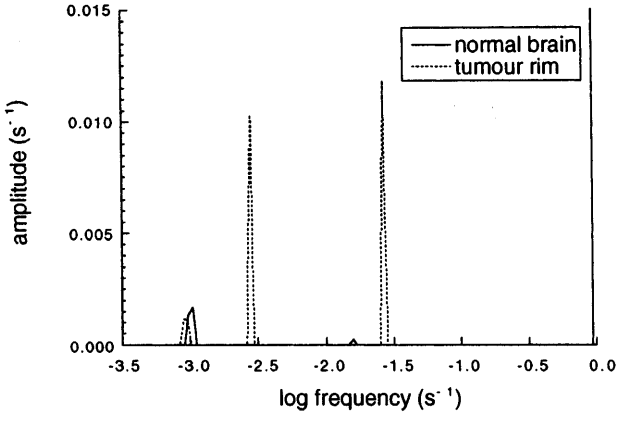

(c)

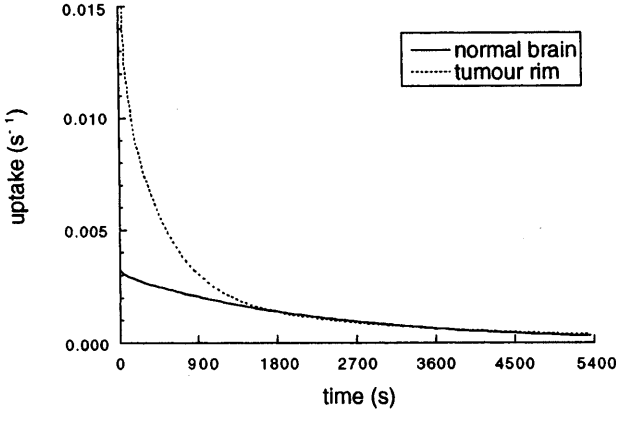

(d)

Fig. 2 **a** Image taken from a [^{11}C]-temozolomide PET study, showing the accumulated drug (at tracer levels) detected in tumour and normal brain over a 90-min period. **b** Time-activity curves corresponding to tumour rim, normal brain and arterial plasma. **c** Spectrum of kinetic components obtained by spectral analysis of the curves shown in **b. d** Corresponding impulse response functions

Table 2 Pharmacokinetic parameter estimates for the [^{11}C]-temozolomide study

	Normal grey matter	Tumour
VD	6.97	54.4
K_1 (s^{-1})	0.003	0.024
MRT (s)	2141	2236
$t_{1/2z}$ (s)	1598	1932

Estimated pharmacokinetic parameters for this population sample reveal that acridine carboxamide has a large volume of distribution in the liver, kidney and spleen and prolonged retention in the liver and spleen as compared with other organs, as indicated by increased MRT and $t_{1/2z}$ values. By comparison, this drug has a markedly lower volume of distribution in the brain versus other organs, mainly due to low initial uptake (K_1) and only moderate retention. Tumour uptake is initially low but retention is relatively prolonged.

Predicting drug handling by tumours

The predicted tumour handling in response to a constant infusion of 5-[^{18}F]-FU is shown in Figs. 4a and 4b. The graphs indicate that 5-[^{18}F]-FU does not reach steady state in the tumour within the period of the PET study (90 min). Our analysis indicates that it takes approximately 10 h for the drug concentration in the tumour to reach a plateau value, and at that time it achieves an approximately 10-fold higher concentration of 5-[^{18}F]-FU than does plasma. By definition, this is the fractional volume of distribution of the drug in tumour. However, these results give only an indication of the time required to reach steady state and an approximate value for the

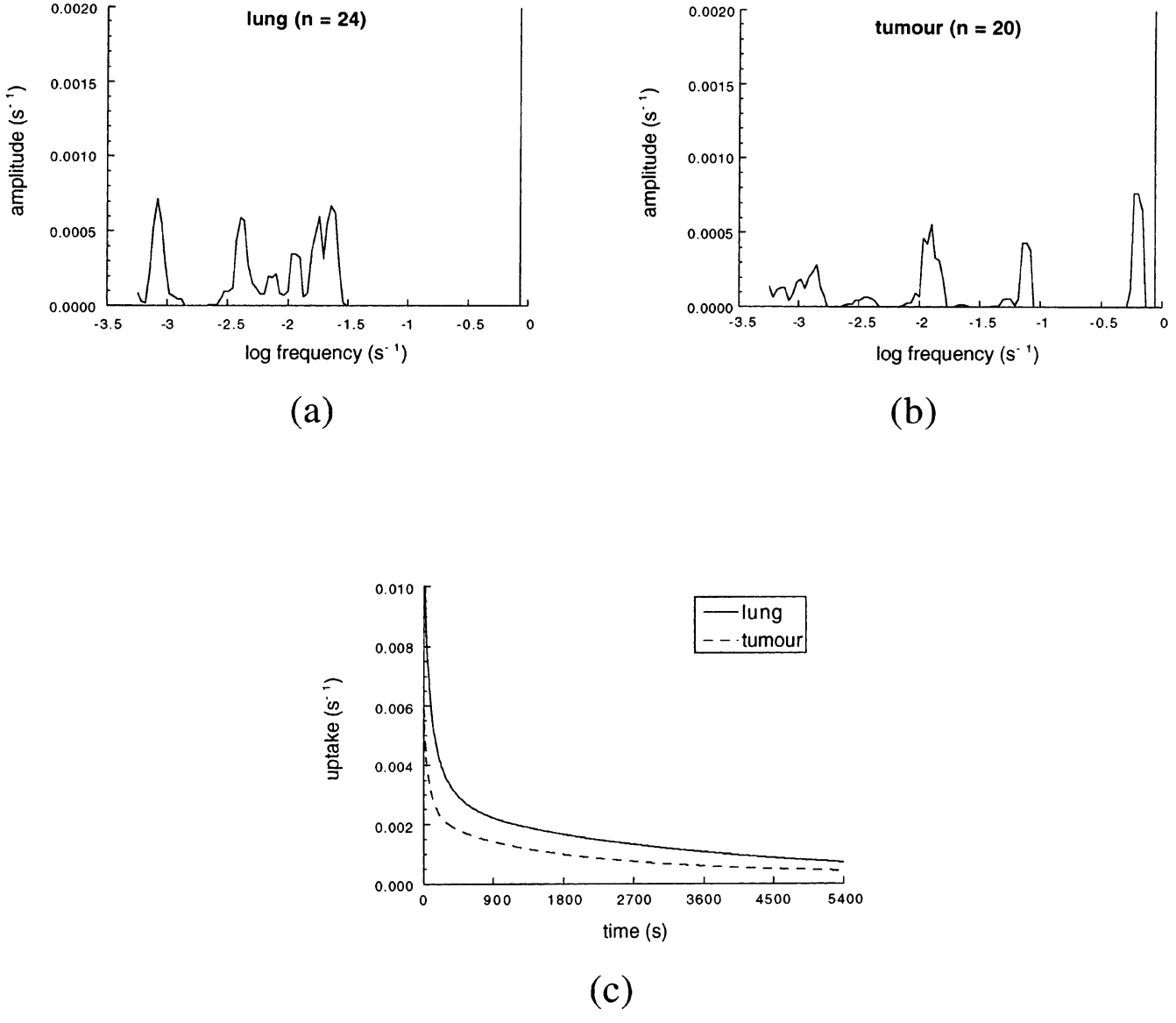

Fig. 3 **a** Average of lung parenchyma spectra obtained from 24 individuals undergoing [^{11}C]-acridine carboxamide PET studies. **b** Average of 20 tumour spectra obtained from the same population of patients. **c** Impulse response functions representing the average expected kinetic behaviour of [^{11}C]-acridine carboxamide in lung and tumour

volume of distribution, since parameter estimates become increasingly unreliable when extrapolated beyond the duration of the PET study (see Discussion).

Parametric images of pharmacokinetic variables

Images of the impulse response at 1 and 60 min and of *VD* are shown for the [^{11}C]-temozolomide study in Figs. 5a, 5b, and 5c, respectively. The 1-min image indicates markedly increased uptake of tracer from plasma by the tumour rim as compared with the surrounding grey matter. The late image shows that despite the marked differences in tracer delivery, retention of [^{11}C]-temozolomide in the tumour is very similar to that in the

Table 3 Group-average pharmacokinetic parameter estimates for [^{11}C]-acridine carboxamide

	Liver (n = 7)	Kidney (n = 9)	Spleen (n = 5)	Lung (n = 24)	Brain (n = 4)	Tumour (n = 20)
VD	858	680	804	131	20.6	203
K_1 (s^{-1})	0.007	0.017	0.015	0.011	0.004	0.007
MRT (s)	120741	40654	55208	11628	4792	31247
$t_{1/2z}$ (s)	2443	221	1230	71.2	734	1376

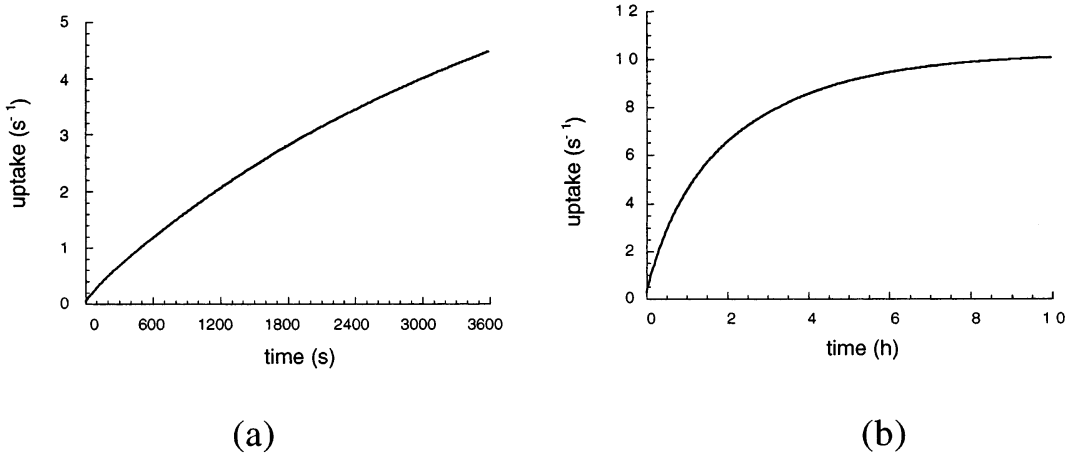

Fig. 4 **a** Predicted drug handling by a tumour in response to a constant infusion of 5-FU. **b** The same tumour response curve shown with an expanded time axis, indicating that 5-FU takes up to 10 h to reach steady state in the tumour

surrounding grey matter, suggesting a similar degree of binding. It follows, then, that the *VD* image is dominated by the delivery phase of tracer uptake. The parametric images are in good agreement with the ROI analysis of the same study shown in Fig. 1.

Together, the ROI analysis and the parametric images suggest that factors affecting the initial uptake of temozolomide from the plasma pool may be important determinants of the efficacy of the drug in human brain tumours. There is also a suggestion (ROI analysis), of prolonged retention in tumour, but this cannot be concluded from a single-patient study.

Discussion

In this report we describe the use of spectral analysis of PET data for the pharmacokinetic assessment of labeled anti-cancer drugs. Spectral analysis produces parameter estimates with slightly higher bias and variance than does an idealised compartmental model, but without assuming a fixed number of tissue compartments. We also demonstrate that spectral analysis provides useful kinetic information about new drugs when applied to either an individual PET study or pooled data. The technique can also be used to predict tissue handling in response to different drug administration protocols, provided that the assumption of linear kinetics holds (see below), and to produce functional parametric images describing the kinetic and spatial distribution of a labeled drug in vivo. It should be emphasised that similar kinetic information about the developmental drugs used in this study cannot easily be obtained by conventional techniques due to the lack of prior knowledge about drug handling in vivo.

The use of fewer assumptions in the spectral analysis technique gives rise to some important advantages over conventional approaches for analysis of tracer kinetic data, particularly in tumours. For example, compartmental models assume homogeneous tissue kinetics within the sampled ROI, which is unlikely to be the case in tumours, resulting in biased parameter estimates [12, 20]. The spectral analysis model is not restricted by this assumption. Indeed, it was originally explored as a potential tool for assessment of kinetic heterogeneity in PET studies [9]. In the presence of a heterogeneous mix of tissues the estimated unit impulse response (and any derived parameter, such as volume of distribution) is the average of all tissues sampled in the ROI, weighted by their relative contributions. However, in the interpretation of spectra it must be recognised that, as a result of heterogeneity, the number of peaks may not correspond

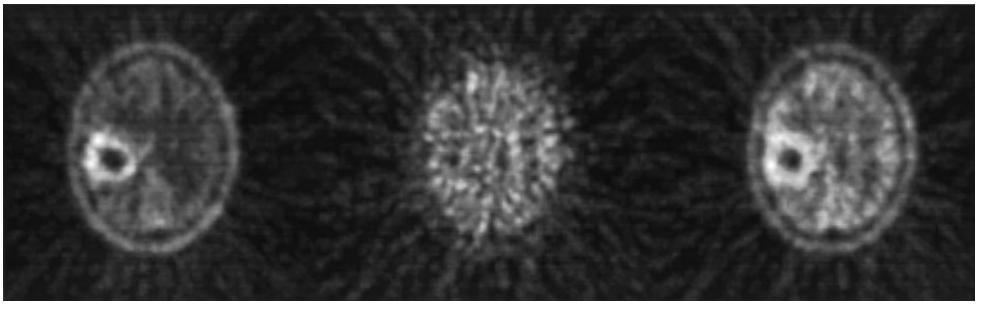

Fig. 5a–c Functional parametric images of [^{11}C]-temozolomide, demonstrating **a** the impulse response at 1 min (approximately equivalent to K_1), **b** the impulse response at 60 min (indicating drug binding) and **c** the volume of distribution

to the number of discrete tissue compartments. For example, the presence of three peaks in the tumour spectrum obtained for [^{11}C]-temozolomide (Fig. 2c) may indicate heterogeneity of kinetic behaviour rather than three physiological compartments. Alternatively, there may actually be three compartments for both tumour and normal brain, but due to the noise and similarity of kinetics in two of the three compartments in normal brain, these dynamics cannot be resolved.

Although the examples presented in this report involve compounds labeled with positron emitters, the use of spectral analysis is not restricted to PET data. Tracer studies are commonly performed using single-photon emitters, and recent advances in chemistry and instrumentation make it feasible to perform quantitative labeled-drug studies using single-photon tomography. Spectral analysis is equally applicable to such studies. The technique is also applicable to non-imaging studies such as measurements of plasma drug clearance. Indeed, the technique originally derived from an approach to the analysis of enzyme binding potentials in vitro [25].

Limitations of spectral analysis

Although spectral analysis has many useful applications in tracer kinetics studies, there are some limitations to the technique that may affect interpretation of the results. It is noteworthy, however, that these problems are germane to most modeling techniques, including compartmental modeling, and are not unique to spectral analysis. The main limitations are due to (a) statistical noise, (b) errors in the measured arterial input function and (c) non-linear kinetics.

Noise

The presence of statistical noise in the measured data can give rise to spurious peaks, particularly at the extreme ends of the spectrum. This is demonstrated in Fig. 6, which shows the average of 1000 spectra individually produced by analysis of the same simulated tissue curve shown in Fig. 1a, but with different noise being added each time. The build-up towards either end of the spectrum occurs when the NNLS algorithm attempts to fit the noise in the data. Therefore, the presence of peaks in these regions should be interpreted with caution. The problem also manifests as increased errors in estimation of the intercept and terminal slope of the unit impulse-response function, which mainly affects estimates of K_1 and *MRT*. In addition, parametric images, such as the ones calculated for temozolomide (Fig. 5), are more susceptible to noise than is fitting of ROI data. This is because the signal-to-noise ratio in a given ROI sample decreases approximately as the square of the number of pixels in the ROI (and a single pixel is the smallest possible ROI). Despite this, it is possible to obtain useful spatial as well as kinetic information with the pixel-by-pixel fitting approach. In some cases, depending on the particular tracer involved and on the counting efficiency of the tomograph, it may be necessary to apply a penalty term to the cost function of Eq. 4 to obtain good-quality parametric images [6, 10]. For example, one can penalise values of α that occur in parts of the spectrum that are relatively more sensitive to noise, such as the extrema. This was not necessary in the temozolomide case. The problem of estimating kinetic parameters from noisy data is compounded by the use of ^{11}C in many PET studies because of its relatively short half-life (20.4 min). This results in a poor signal-to-noise ratio in measurements taken towards the end of the study and limits the time course over which data can be recorded. This, in turn, affects the ability of spectral analysis and other modeling techniques to estimate reliably parameters relating to tracer retention.

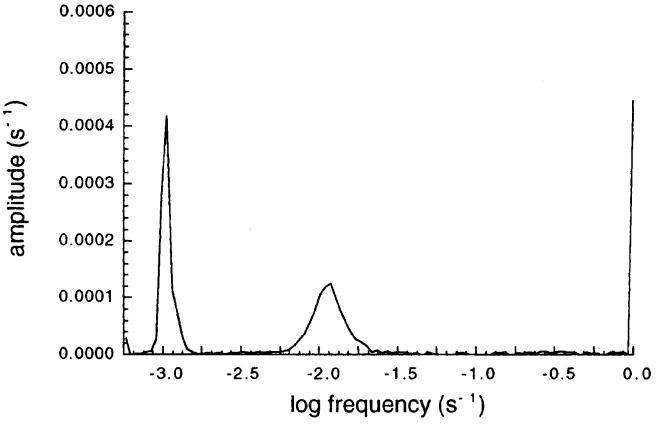

Fig. 6 Average of 1000 spectra individually obtained by spectral analysis of the simulated time-activity curve shown in Fig. 1a, but with different noise being added each time

Input function errors

Problems can occur if the measured arterial input function is different from the actual input seen by the tissue of interest. For example, the delivered bolus takes approximately 15 s longer to reach the sampling point at the radial artery catheter than it does to reach the tissue of interest and is often somewhat more dispersed [13]. Although the delay is small, it can cause problems in estimation of fast dynamics and a poor fit to the early uptake phase of the time-activity curve. This may explain the secondary peak adjacent to the blood volume peak at the extreme right of the average spectrum obtained for [^{11}C]-acridine carboxamide (Fig. 3b). However, delay and dispersion can be accounted for in the model and have minimal impact on intermediate and slow dynamics, which are often of greater interest. In some cases the input function may be different for different organs in the field of view. For example, the liver takes its blood supply from both portal vein and the

hepatic artery, whereas other tissues, including liver metastases, receive mainly arterial blood. Thus, the use of an arterial input function may result in biased parameter estimates for the liver.

Further problems occur if the chosen input function does not accurately reflect the presence of labeled compounds that freely exchange with the tissue space and when significant concentrations of labeled metabolites contribute to the PET signal. These problems arise because of the inability of PET to distinguish different chemical forms of the labeled compound (parent versus metabolite, free versus protein-bound), which is one of the main drawbacks of the PET technique. For example, [^{11}C]-acridine carboxamide is highly protein-bound (>95% [17]), which may explain the long tail we typically observe in these input functions. However, only 'free' parent can cross the capillary membranes to enter the tissue space, suggesting that this tail should not be used. If the tail does indeed represent protein-bound drug, then its inclusion in the input function would cause an underestimation of the terminal half-lives in our analysis. Another possible source of error occurs in the case of 5-[^{18}F]-FU, where all the label in plasma is attributed to labeled fluorobeta-alanine (FBAL) after a few minutes. Hence, it is likely that [^{18}F]-FBAL is a major contaminating factor. However, as the initial increase in tissue signal occurs during the period when FBAL has not yet appeared in plasma and as the metabolite is not expected to be taken up into cells, it is anticipated that the main contribution to the PET signal in tumour is that of labeled 5-[^{18}F]-FU. Hence, we believe that 5-[^{18}F]-FU in plasma is the most appropriate input function in this case. However, the exact choice of input function may be tissue-dependent, as FBAL may be taken up into some cells such as renal parenchyma. Similarly, the labeled parent drug is used for the input function in temozolomide studies, as the main metabolite detected in plasma is more polar than temozolomide and, therefore, less likely to cross the blood-brain barrier (BBB). However, this assumption may break down when BBB disruption occurs in brain tumours. It should be noted that these problems are common to other methods of analysis such as compartmental modeling.

Non-linear kinetics

The 5-[^{18}F]-FU example demonstrates the use of spectral analysis to predict drug handling in response to any given input function and extrapolation to therapeutic dose levels. However, this is valid only under the assumption of linear kinetics. If there are saturable processes involved in the uptake and retention of the drug in tissue, the rates of exchange between compartments are no longer constant but vary with time, depending on the availability of binding sites and/or metabolising enzymes. In these circumstances the assumption of linear kinetics breaks down and the results obtained with a tracer study cannot be extrapolated to therapeutic levels. It may, however, be possible to model saturation kinetics within the spectral analysis framework using an alternative set of bases to exponentials, but we did not explore this possibility in the present work. It is also important that one note potential problems in extrapolation of data beyond the duration of the PET study as illustrated in the 5-[^{18}F]-FU example. Clearly, the further data are extrapolated beyond the last measurement, the less reliable they become. This should be borne in mind in the interpretation of predicted tissue responses, including impulse response functions. In other words, estimates of *VD* (and, hence, *MRT*) and the time taken to reach steady state are reliable if steady state is achieved during the PET study but are less so for more slowly equilibrating tissues.

The problems mentioned above mainly affect the interpretation of individual spectra, whereas the estimated unit impulse-response function provides a reasonably robust description of regional tissue kinetics, provided that the input function is a good approximation to that seen by the tissue of interest as discussed above. Furthermore, whereas the interpretation of individual patients spectra is affected by heterogeneity, noise and transient vascular effects, conclusions can be drawn from average spectra with reasonable confidence as demonstrated by the acridine carboxamide data. Thus, the group average approach is a useful way to characterise the kinetic behaviour of a drug in vivo and may provide sufficient information for construction of a compartmental model for more detailed analysis.

In summary, spectral analysis provides a relatively straightforward means of obtaining kinetic information similar to that obtained by more highly constrained models. Furthermore, because the technique makes relatively few assumptions, it can be applied to a wide variety of labeled compounds and is less prone to bias than the traditional compartmental modeling approach. Therefore, spectral analysis will be an important tool in the evaluation of novel anti-cancer drugs using PET. The technique is being further refined to improve the reliability of parameter estimates in the presence of noise and to improve the signal-to-noise of functional parametric images.

Acknowledgements This work was supported by the UK Cancer Research Campaign (CRC grant SP2 193/0101). Temozolomide was developed by the CRC and is now licensed to Schering-Plough. The authors would like to thank the chemistry staff of the MRC Cyclotron Unit for the preparation and metabolite analysis of the radiolabeled drugs.

References

1. Atwell GJ, Rewcastle GW, Baguley BC (1987) Potential antitumour agents. 50. In vivo solid tumour activity of derivatives of *N*-[2-(dimethylamino)ethyl]acridine-4-carboxamide. J Med Chem 30: 664–669
2. Bailey DL, Meikle SR (1994) A convolution-subtraction scatter correction method for 3D PET. Phys Med Biol 39: 411–424

3. Brock CS, Matthews JC, Brown G, Luthra SK, Brady F, Newlands ES, Price P (1996) The kinetic behaviour of temozolomide in man. J Clin Oncol 15: 475
4. Brown GD, Turton DR, Luthra SK, Osman S, Waters SL, Harte RJA, Tilsley DWO, Price PM, Jones T, Denny WA, Brady F (1994) Carbon-11 labelling of the antitumour agent, [*N*-^{11}C-methyl]NSC 601316 for pre-clinical evaluation in man by PET. J Labelled Compd Radiopharm 35: 558
5. Brown GD, Turton DR, Luthra SK, Price P, Jones T, Stevens MFG, Baghurst DR, Mingos DMP, Osman S, Walters SL, Brady F (1994) Synthesis of [^{11}C-methyl]methylisocyanate and application with microwave heating to labelling the novel anticancer agent temozolomide. J Labelled Compd Radiopharm 35: 100–102
6. Chiao P, Fessler JA, Zasadny KR, Wahl RL (1995) Spectral analysis using regularized non-negative least-squares estimation. Conference record of the 1995 IEEE medical imaging conference, San Francisco, 21–28 October 1995, pp 1680–1683
7. Collins JM, Dedrick RL, King FG, Speyer JL, Myers CE (1980) Nonlinear pharmacokinetic models for 5-fluorouracil in man: intravenous and intraperitoneal routes. Clin Pharmacol Ther 28: 235–246
8. Cunningham VJ, Jones T (1993) Spectral analysis of dynamic PET studies. J Cereb Blood Flow Metab 13: 15–23
9. Cunningham VJ, Bailey DL, Hutton B, Richardson A, Jones T (1991) A practical method for assessing heterogeneity in kinetic PET data. J Cereb Blood Flow Metab 11 [Suppl 2]: S558
10. Cunningham VJ, Ashburner J, Byrne H, Jones T (1993) Use of spectral analysis to obtain parametric images from dynamic PET studies. In: Uemura K, Lasson NA, Jones T, Kanno I (eds) Quantification of brain function. Tracer kinetics and image analysis in brain PET. Elsevier, Amsterdam, pp 101–108
11. Harte RJA (1996) Pharmacokinetic evaluation of anticancer drugs using positron emitting nuclides. MD Thesis, University of Bristol
12. Herholz K, Wienhard K, Heiss W-D (1990) Validity of PET studies in brain tumours. Cerebrovasc Brain Metab Rev 2: 240–265
13. Iida H, Higano S, Tomura N, Shishido F, Kanno I, Miura S, Murakami M, Takahashi K, Sasaki H, Uemura K (1988) Evaluation of regional differences in tracer appearance time in cerebral tissues using [^{15}O]water and dynamic positron emission tomography. J Cereb Blood Flow Metab 8: 285–288
14. Kinahan PE, Rogers JG (1989) Analytic 3-D image reconstruction using all detected events. IEEE Trans Nucl Sci 36: 964–968
15. Lawson CL, Hanson RJ (1974) Solving least squares problems. Prentice-Hall, Englewood Cliffs, New Jersey
16. Matthews JC, Bailey D, Price P, Cunningham V (1997) The direct calculation of parametric images from dynamic PET data using maximum-likelihood iterative reconstruction. Phys Med Biol 42: 1155–1173
17. Paxton JW, Young D, Robertson IGC (1993) Pharmacokinetics of acridine-4-carboxamide in the rat, with extrapolation to humans. Cancer Chemother Pharmacol 32: 323–325
18. Ramachandran GN, Lakshminarayanan AV (1971) Three-dimensional reconstruction from radiographs and electron micrographs: application of convolutions instead of Fourier transforms. Proc Natl Acad Sci USA 68: 2236–2240
19. Ranicar ASO, Williams CW, Schnorr L, Clark JC, Rhodes CG, Bloomfield PM, Jones T (1991) The on-line monitoring of continuously withdrawn arterial blood during PET studies using a single BGO/photomultiplier assembly and non-stick tubing. Med Prog Technol 17: 259–264
20. Schmidt K, Lucignani G, Moresco RM, Rizzo G, Gilardi MC, Messa C, Colombo F, Fazio F, Sokoloff L (1992) Errors introduced by tissue heterogeneity in estimation of local cerebral glucose utilization with current kinetic models of the [^{18}F]fluorodeoxyglucose method. J Cereb Blood Flow Metab 12: 823–834
21. Spinks TJ, Jones T, Gilardi MC, Heather JD (1988) Physical performance of the latest generation of commercial positron scanners. IEEE Trans Nucl Sci 35: 721–725
22. Spinks TJ, Jones T, Bailey DL (1992) Physical performance of a positron tomograph for brain imaging with retractable septa. Phys Med Biol 37: 1637–1655
23. Stevens MFG, Hickman JA, Langdon SP (1987) Antitumour activity and pharmacokinetics in mice of 8-carbamoyl-3-methyl-imidazo [5,1-*d*]-1,2,3,5-tetrazin-4 (3H)-one (CCRG 91045; M&B 39831), a novel drug with potential as an alternative to dacarbazine. Cancer Res 47: 5846–5852
24. Tilsley DWO, Harte RJA, Jones T, Brady F, Luthra SK, Brown G, Price PM (1993) New techniques in the pharmacokinetic analysis of cancer drugs. IV. Positron emission tomography. Cancer Surv 17: 425–442
25. Tobler HJ, Engel G (1983) Affinity spectra: a novel way for the evaluation of equilibrium experiments. Naunyn-Schmiedebergs Arch Pharmacol 322: 183–192
26. Wells P, Harte RJA, Price P (1996) Positron emission tomography: a new investigational area for cancer research. Clin Oncol 8: 7–14